Investigation of Multiple Rectangular Aperture Irises in Rectangular Waveguide Using TE^x_{mn}-Modes

Rong Yang and A. S. Omar, *Senior Member, IEEE*

Abstract—**With the use of proper aperture basis functions in conjunction with the moment method and TE^x_{mn}-modal expansion, the coupling effect of transverse irises with multiple rectangular coupling apertures in a rectangular waveguide has been investigated. Numerical studies carried out for twin- and triple-aperture coupling irises have been confirmed by the experiments. The simulation result for a Ka-band bandpass filter realized with triple-aperture irises gives a higher stop-band attenuation than that of a filter with single-aperture irises. The use of TE^x_{mn}-modal expansion is characterized by the reduction of both computer memory and CPU time requirements during the numerical study as compared with the commonly used $TE_{mn} - TM_{mn}$ modal approach.**

I. INTRODUCTION

WAVEGUIDE iris coupling plays an important role in waveguide filters and impedance matching networks. The coupling with single-aperture irises has been extensively studied by using different methods [1]–[6]. Multiaperture coupling irises with either purely inductive or capacitive apertures have been treated by various authors in the past [7]–[9]. For coupling irises with neither purely inductive nor capacitive multiple apertures, the problem was seldomly touched. Masterman *et al.* [10] have proposed a method to solve this problem in principle without performing a numerical study.

When a TE_{10}-mode is incident on a transverse plane coupling iris in a rectangular waveguide, both TE_{mn}- and TM_{mn}-modes can be excited. But field computation using $TE_{mn} - TM_{mn}$ modal approach indicates that, with a TE_{10}-mode incidence, the excited E_x in the iris plane is either zero or very small independent of the aperture geometry. Thus, by neglecting this zero or tiny E_x field, namely by using TE^x_{mn}-modal expansion to represent the waveguide field, which automatically excludes the E_x component, no significant error will be introduced. Compared to the use of $TE_{mn} - TM_{mn}$-modal approach, where many higher order modes must be included to model a zero or very small E_x field, the use of less TE^x_{mn}-modes results in up-speeding the numerical calculations and reducing of computer memory.

The TE^x_{mn}-mode approach has been successfully used by Bornemann *et al.* [11] to analyze waveguide step discontinuities with the mode matching method. Here we apply this approach in conjunction with the moment method to analyze the coupling by multi aperture irises in the transverse plane of a rectangular waveguide. The validity of the theoretical analysis has been confirmed by experiment for twin- and triple-aperture coupling irises.

Manuscript received August 31, 1992; revised January 4, 1993.
The authors are with the Arbeitsbereich Hochfrequenztechnik, Technische Universität Hamburg-Harburg, 21071 Hamburg, Germany.
IEEE Log Number 9035408.

II. THEORY

The structure under consideration is shown in Fig. 1. The coupling iris in the transverse plane of a rectangular waveguide contains N different rectangular apertures. The iris itself is assumed to be infinitesimally thin and perfectly conducting. The size of the jth aperture is $a^j_o \times b^j_o$.

In case of TE^x_{mn}-modal representation, the transverse electromagnetic field in region $i = 1, 2$ (at each side of the coupling iris) are derived from the x-component of a vector potential A_x:

$$\begin{aligned} E_y &= \frac{\partial}{\partial_z} A_x \\ H_x &= \frac{j}{\omega\mu_o}\left[k_o^2 + \frac{\partial^2}{\partial x^2}\right] A_x \\ H_y &= \frac{j}{\omega\mu_o}\frac{\partial^2}{\partial x \partial y} A_x \end{aligned} \tag{1}$$

and

$$\begin{aligned} A_x = 2 \pm \sum_\ell \sqrt{\frac{\omega\mu_o\beta_\ell}{ab(k_o^2 - k_x^2)}}\, T_{mn}(x,y) \\ \cdot \left(V^i_\ell e^{-j\beta_\ell z} - R^i_\ell e^{j\beta_\ell z}\right) \end{aligned} \tag{2}$$

where V^i_ℓ and R^i_ℓ are the wave amplitudes incident to and reflected from the iris. The index ℓ is related to the combination of subscripts (m, n) in the function

$$\begin{aligned} T_{mn}(x,y) &= \sin(k_x x)\cdot\cos(k_y y)/\sqrt{1+\delta_{no}} \\ k_x &= (m\pi/a), \qquad k_y = (n\pi/b) \\ k_o &= f/c \quad \text{and} \quad \beta_\ell = \sqrt{k_o^2 - k_x^2 - k_y^2} \end{aligned} \tag{3}$$

where c is the velocity of light.

The transverse electrical field of the jth aperture is expanded in terms of a set of basis functions

$$\boldsymbol{E}^j_{ap} = \sum_k d^j_k \boldsymbol{e}^j_k. \tag{4}$$

For a rectangular aperture, according to [12], the basis functions may take the following form:

$$e^j_x = \frac{\cos\left[p\pi\left(x - x^j_o\right)/a^j_o\right]}{\sqrt{\left(x - x^j_o\right)\left[1 - \left(x - x^j_o\right)/a^j_o\right]}}$$

$$\cdot \frac{\sin[q\pi(y-y_o^j)/b_o^j]}{\sqrt{(y-y_o^j)\left[1-(y-y_o^j)/b_o^j\right]}}$$

$$e_y^j = \frac{\sin[p\pi(x-x_o^j)/a_o^j]}{\sqrt{(x-x_o^j)\left[1-(x-x_o^j)/a_o^j\right]}} \cdot \frac{\cos[q\pi(y-y_o^j)/b_o^j]}{\sqrt{(y-y_o^j)\left[1-(y-y_o^j)/b_o^j\right]}} \tag{5}$$

where $p, q = 0, 1, 2, \cdots$, and $(p,q) \neq (0,0)$. (x_o^j, y_o^j) are the coordinates of the lower left corner of the jth aperture in the coordinate system as indicated in Fig. 1.(a).

By matching the transverse electric fields in the iris plane to the aperture electric fields and the transverse magnetic fields to each other, the following coupling equations relating the incident and the reflected mode amplitudes can be obtained

$$\begin{aligned}(\underline{V}^1 + \underline{R}^1) &= [\mathrm{C}]\underline{d}\\ (\underline{V}^2 + \underline{R}^2) &= [\mathrm{C}]\underline{d}\\ [\mathrm{K}](\underline{V}^1 - \underline{R}^1) &= [\mathrm{K}](\underline{R}^2 - \underline{V}^2).\end{aligned} \tag{6}$$

Each of the matrices [C] and [K] is composed of N sub matrices as

$$[\mathrm{C}] = [[\mathrm{C}^1], \cdots, [\mathrm{C}^j], \cdots, [\mathrm{C}^N]] \quad \text{and}$$

$$[\mathrm{K}] = \begin{bmatrix} [\mathrm{K}^1] \\ \vdots \\ [\mathrm{K}^j] \\ \vdots \\ [\mathrm{K}^N] \end{bmatrix} \tag{7}$$

with jth sub matrix element defined by

$$\mathrm{C}_{\ell k}^j = \frac{\int_{\mathrm{S}^j} \boldsymbol{E}_\ell^* \cdot \boldsymbol{e}_k^j \, ds}{\int_{\mathrm{S}} \boldsymbol{E}_\ell^* \cdot \boldsymbol{E}_\ell \, ds} \tag{8}$$

$$\mathrm{K}_{k\ell}^j = \int_{\mathrm{S}^j} \boldsymbol{e}_k^j \cdot (\boldsymbol{H}_\ell \times \boldsymbol{z}) \, ds$$

where $\boldsymbol{E}_\ell$ and $\boldsymbol{H}_\ell$ are the dielectric and magnetic field, respectively, corresponding to the ℓth waveguide mode, S^j is the area of the jth aperture, S the cross-section of the rectangular waveguide and $\boldsymbol{z}$ is the unit vector in $\boldsymbol{Z}$-direction. The column vectors V^1, R^1, V^2, R^2, and d have the elements $V_\ell^1, R_\ell^1, V_\ell^2, R_\ell^2$, and d_k, respectively.

After some mathematical manipulations, the modal scattering matrices describing the multiple-aperture iris coupling are derived out

$$\begin{aligned}[\mathrm{S}_{11}] &= [\mathrm{C}]([\mathrm{C}][K])^{-1}[\mathrm{K}] - [\mathrm{U}],\\ [\mathrm{S}_{21}] &= [\mathrm{C}]([\mathrm{C}][K])^{-1}[\mathrm{K}],\\ [\mathrm{S}_{12}] &= [\mathrm{S}_{21}], \qquad [\mathrm{S}_{22}] = [\mathrm{S}_{11}].\end{aligned} \tag{9}$$

where [U] is a unit matrix.

Unlike in [11], where the matrix related to the magnetic field is formed partly by matching the component H_x of the TE_{mo}^x-modes and the rest by matching the H_y component of TE_{mn}^x-modes $(n \neq 0)$, we consider here both magnetic field components as a whole and add the respective parts together to form the matrix [K].

The number of basis functions for each aperture can be chosen to be the same or to be different according to their geometries. By considering their relative geometries, the size of the matrices in (6) can be reduced. When the two apertures, say jth and j_1th, are identical and symmetrically located in the waveguide transverse plane, the same number of basis functions can be used for each aperture. In this case, the elements of the submatrices $[C^{j_1}]$ and $[K^{j_1}]$ can be absorbed into the jth submatrices as:

$$\mathrm{C}_{\ell k}^j = \mathrm{C}_{\ell k}^j + \mathrm{C}_{\ell k}^{j_1} \quad \text{and} \quad \mathrm{K}_{k\ell}^j = \mathrm{K}_{k\ell}^j + \mathrm{K}_{k\ell}^{j_1}$$

and then the j_1th submatrices can be dropped out from the overall matrices. If the whole iris structure is symmetrical, for the TE_{10}-mode incidence the excited higher order TE_{mn}^x-modes in the vicinity of the iris can only be such with m being odd number and n even number. The utilization of these two facts can further reduce the computer storage requirement and speed up the numerical solution.

III. Numerical and Experimental Results

Numerical and experimental studies were carried out in X-band for various coupling irises with twin- and triple-apertures. For the experiment, the coupling irises were made from a 0.1 mm thick copper sheet. The measured scattering parameters were converted into normalized shunt susceptance according to

$$\overline{\mathrm{B}} = -\frac{2\sin\Phi}{|S_{21}|}$$

where Φ is the phase angle of S_{21}. The investigation were confined to symmetrical irises.

A. Single-Aperture Iris

In order to demonstrate the validity and advantages of the TE_{mn}^x-approach single-aperture iris was first studied. Fig. 2 gives the normalized shunt susceptanc for a single-aperture iris from both TE_{mn}^x-and $\mathrm{TE}_{mn} - \mathrm{TM}_{mn}$-method, together with the measured data. Excellent agreement of the three results is obvious. In the calculation, $m \leqslant 40$ and $n \leqslant 20$ were used for both cases. Table I reveals the CPU time and memory requirements of the numerical study for 30 frequency points from 8 GHz to 12 GHz on a Convex computer. The reduction of both CPU time and memory by using TE_{mn}^x-approach is evident.

B. Twin-Aperture Iris

The symmetrical twin-aperture iris can be with either two vertical slots or two horizontal slots. Fig. 3(a) shows the normalized shunt susceptance for different horizontal twin-aperture irises as function of the operating frequency. Like the single-aperture iris, the normalized susceptance decreases with frequency. Fig. 3(b) depicts the normalized susceptance versus the interaperture distance D. It is noted that as D becomes

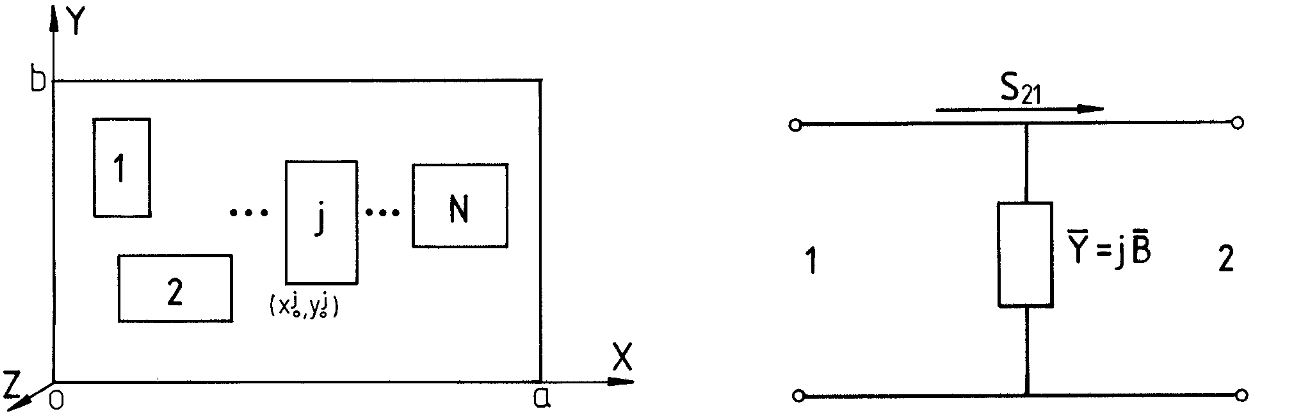

(a) (b)

Fig. 1. Transverse coupling iris with multiple rectangular apertures in a rectangular waveguide. (a) Cross-section view. (b) Equivalent circuit.

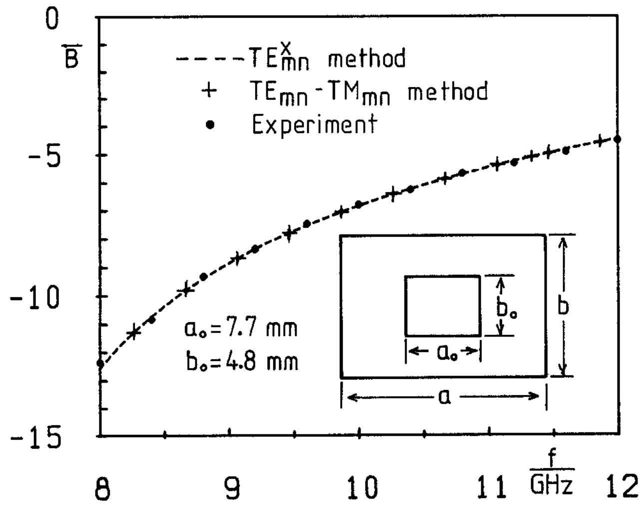

Fig. 2. Normalized susceptance for single-aperture iris.

TABLE I
CPU TIME AND MEMORY REQUIREMENT FOR TE^x_{mn} AND $TE_{mn} - TM_{mn}$ METHODS

	TE^x_{mn}-method	$TE_{mn} - TM_{mn}$-method
CPU Time (s)	5.27	19.52
Memory (Mb)	1.68	3.35

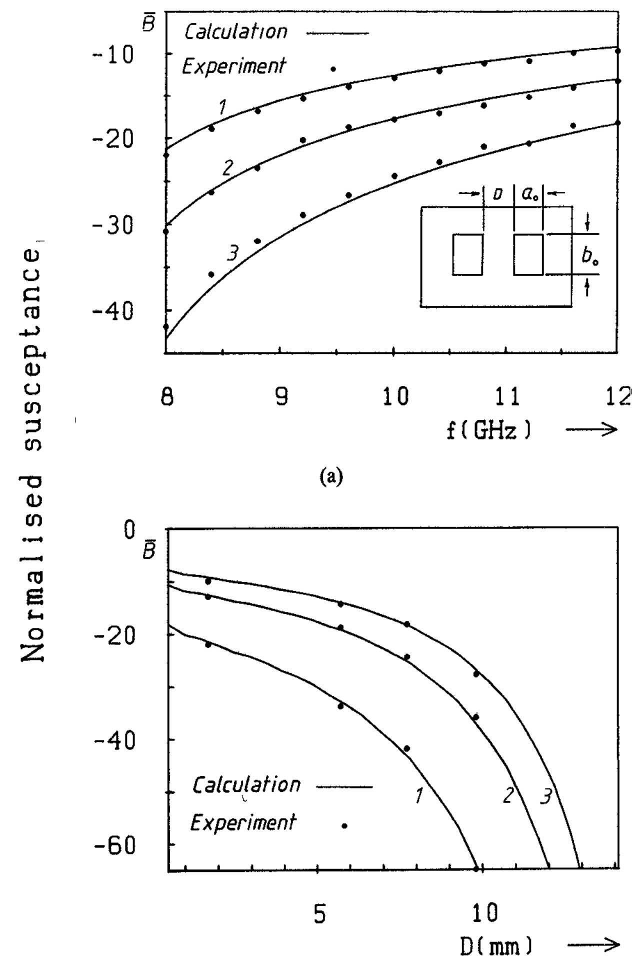

(b)

Fig. 3. Vertical twin-aperture iris. (a) Normalized susceptance versus frequency: (1) $a_o, b_o, D = 4.10, 8.00, 1.70$ mm (2) $a_o, b_o, D = 3.80, 7.80, 3.90$ mm (3) $a_o, b_o, D = 4.10, 8.00, 4.20$ mm. (b) Normalized susceptance versus aperture separation: $a_o, b_o = 4.10, 8.00$ mm (1) f = 8.00 GHz, (2) f = 10.00 GHz, (3) f = 12.00 GHz.

bigger the normalized susceptance reaches a higher value. Excellent agreement between numerical and experimental results can be observed.

For the horizontal twin-aperture iris, Fig. 4(a), the frequency dependence of the normalized susceptance is similar to that of the vertical one. But for the interaperture separation dependence in Fig. 4(b), we can note a quite different pattern as compared to Fig. 3(b). All the curves here have a profile symmetrical to the midvalue point of D. As the distance between the two apertures increases, the normalized susceptance first begins to increase to a certain point, and then it starts to decline as D increases. Here again, the numerical results agree well with the experiments.

For the case of a horizontal twin-aperture iris, when each aperture is narrow in y-direction and sufficiently long in the x-direction, resonance can occur in the operating frequency band. Fig. 5 demonstrates this phenomenon. Curve 1 which

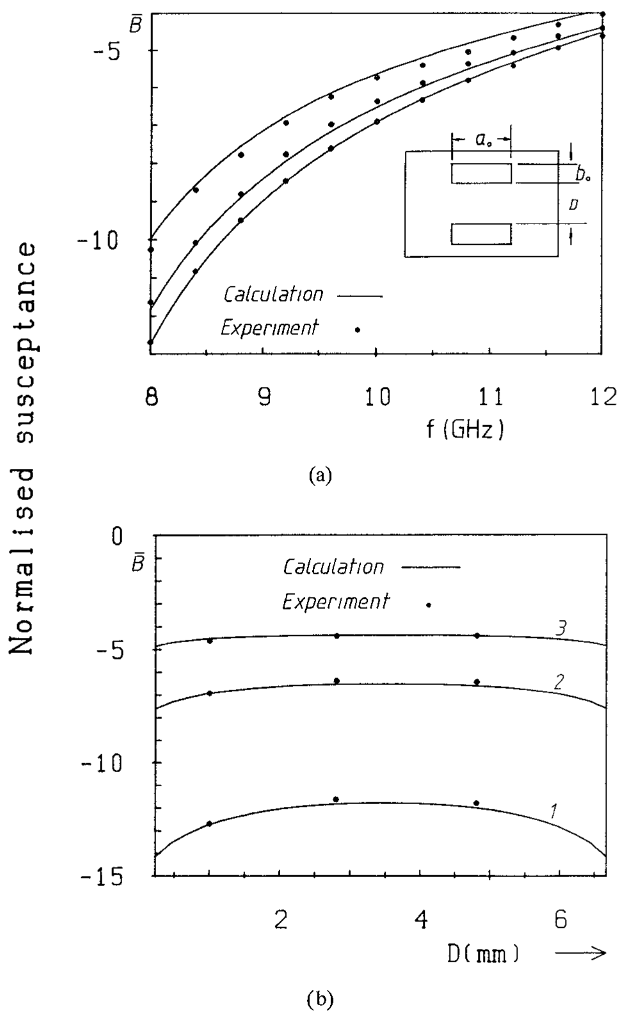

Fig. 4. Horizontal twin-aperture iris. (a) Normalized susceptance versus frequency: (1) $a_o, b_o, D = 7.50, 3.00, 1.90$ mm (2) $a_o, b_o, D = 7.70, 1.80, 2.80$ mm (3) $a_o, b_o, D = 7.70, 1.80, 1.00$ mm. (b) Normalized susceptance versus aperture separation: $a_o, b_o = 7.70, 1.80$ mm (1) f = 8.00 GHz, (2) f = 10.00 GHz, (3) f = 12.00 GHz.

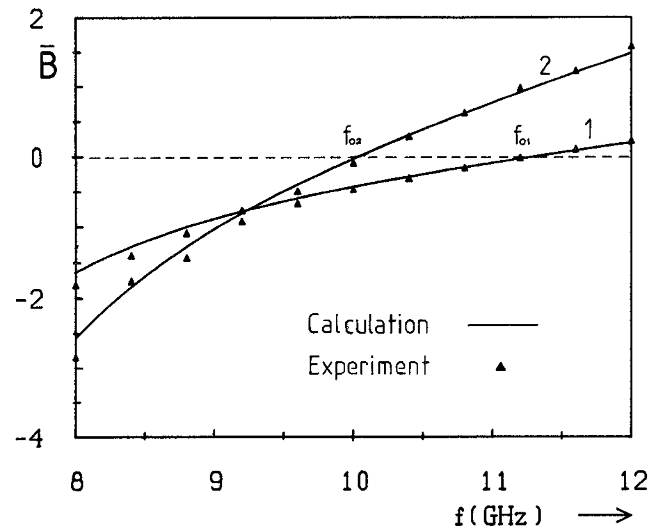

Fig. 5. Normalized susceptance for horizontal twin-aperture resonance iris $a_o, b_o, D = 14.80, 1.00, 1.80$ mm. (1) Both apertures exist. (2) Only one aperture exists.

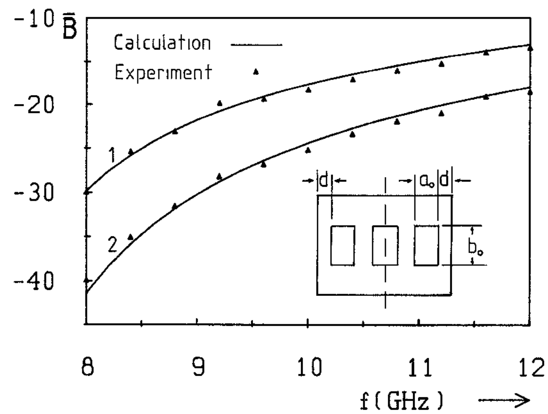

Fig. 6. Normalized susceptance for triple-aperture iris: (1) $a_o, b_o, d = 3.00, 8.00, 4.80$ mm (2) $a_o, b_o, d = 3.20, 8.00, 2.80$ mm.

represents the normalized susceptance when both apertures exist, goes from inductive to capacitive at frequency f_{o1}, while curve 2 is the normalized susceptance with resonance at f_{o2} when one of the apertures disappears. It is clear that the introduction of the second aperture shifts the resonant frequency to a higher value f_{o1}. This second aperture results also in a flatter susceptance curve near resonance which implies a smaller quality factor Q of the resonator.

C. Triple-Aperture Iris

The normalized shunt susceptance of two triple-aperture irises is shown in Fig. 6. Excellent agreement between the numerical and experimental results is demonstrated.

Based on the single iris analyses for both single-aperture and triple-aperture irises two 3-section waveguide bandpass filters with the same midband frequency and bandwidth in Ka-band using triple-aperture irises as shown in Fig. 7(a) and using single-aperture irises as shown in Fig. 2 were synthesized. The corresponding irises for the two filters have the same midband susceptance value. The simulated insertion loss for the two filters are plotted in Fig. 7. It is found that the filter with triple-aperture irises has a few decibel higher attenuation in both lower and upper stopband than its single-aperture counterpart. The geometries of both filters are given in Table II.

IV. Conclusion

Analysis of multiple rectangular aperture iris coupling in rectangular waveguide by using TE^x_{mn}-modal expansion in conjunction with the moment method is presented. The use of TE^x_{mn}-modal expansion which automatically excludes the either very small or zero electric field E_x component results in more than 50% computer storage saving and CPU time reduction down to about 25% as compared with the commonly used $TE_{mn} - TM_{mn}$-approach. Numerical results for various iris structures were confirmed by experiment. A possible application of the multi-aperture iris to the design of waveguide bandpass filter with high stop-band attenuation is suggested.

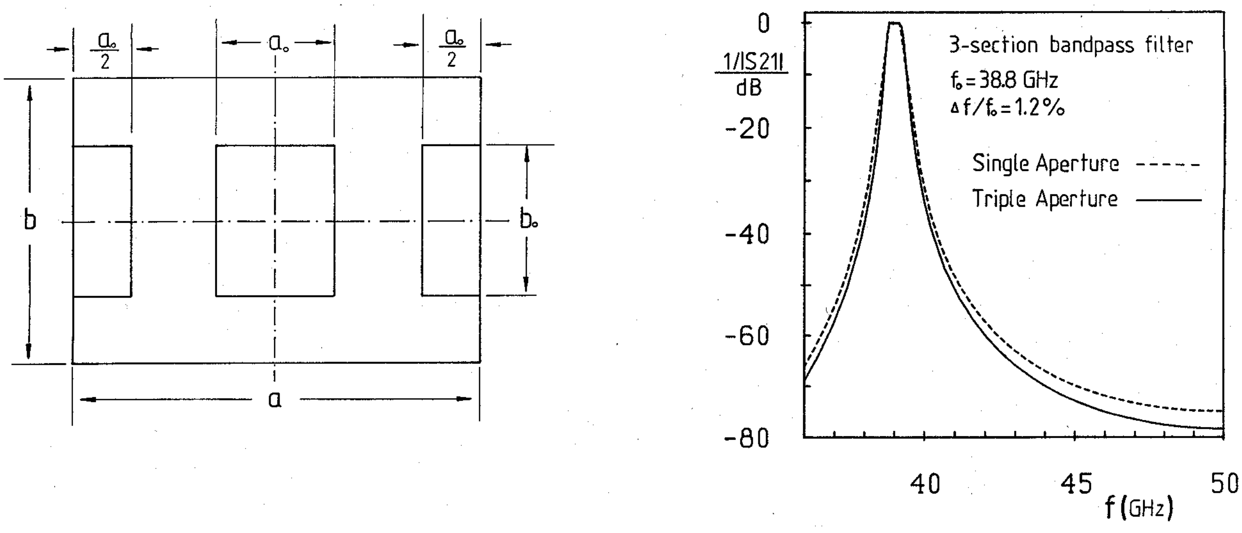

Fig. 7. 3-section Ka-band waveguide bandpass filter: (a) Aperture structure. (b) Filter insertion loss.

TABLE II
KA-BAND 3-SECTION BANDPASS FILTER GEOMETRIES $f_o = 38.8$ GHz $\Delta f/f_o = 1.2\%$ WAVEGUIDE DIMENSION: 7.112 × 3.556 (mm)

Structure	Resonator Length		Aperture Size $a_o \times b_o$(mm)	
	l_1, l_3	l_2	1st and 4th irises	2nd and 3rd irises
Single Aperture	4.339	4.494	1.932 × 2.524	1.032 × 1.934
Triple Aperture	4.301	4.510	1.894 × 3.300	0.760 × 3.300

ACKNOWLEDGMENT

The authors wish to express their gratefulness to Professor Ing. K. Schünemann for his support.

REFERENCES

[1] N. Marcuvitz, *Waveguide Handbook.* New York: McGraw-Hill, 1951.
[2] H. Auda and R.F. Harrington, "A moment solution for waveguide junction problems," *IEEE Trans. Microwave Theory Tech.,* vol. MTT-31, pp. 515–520, 1983.
[3] M.S. Navarro *et al.,* "Propagation in a rectangular waveguide periodically loaded with resonant iris," *IEEE Trans. Microwave Theory Tech.,* vol. MTT-28, pp. 857–865, 1980.
[4] P.S. Kooi *et al.,* "Application of modal analysis to waveguide-cavity junction formed by an iris obstacle," *Proc. Inst. Elec. Eng.,* vol. 131, no. 1, pp. 35–37, Feb. 1984.
[5] H. Patzelt and F. Arndt, "Double-plane step in rectangular waveguide and their applications for transformer, iris, and filter," *IEEE Trans. Microwave Theory Tech.,* vol. MTT-30, pp. 771–776, 1982.
[6] G. Eastham and K. Chang, "Analysis of circular and rectangular apertures in a circular waveguide," *IEEE MTT-S Dig.,* 1990.
[7] S.N. Sinha, "Analysis of multiple-strip discontinuity in a rectangular waveguide," *IEEE Trans. Microwave Theory Tech.,* vol. MTT-34, pp. 696–700, 1986.
[8] B.H. Chu and K. Chang, "Analysis of wide transverse inductive metal strip in a rectangular waveguide," *IEEE Trans. Microwave Theory Tech.,* vol. MTT-37, pp. 1138–1141, 1989.
[9] L. Lewin, "Solution of a singular integral equation over a multiple interval and applications to multiple strips, grids, or waveguide diaphragms," *Electron Lett.,* vol. 2, pp. 458–459, Dec. 1966.
[10] P.H. Mastermann and P.J.B. Clarricoats, "Computer field-matching solution of waveguide transverse discontinuities," *Proc. Inst. Elec. Eng.,* vol. 118, pp. 51–63, 1971.
[11] J. Bornemann and R. Vahldieck, "Characterization of a class of waveguide discontinuities using a modified TE^{x}_{mn}-mode approach," *IEEE Trans. Microwave Theory Tech.,* vol. MTT-38, pp. 1816–1822, 1990.
[12] R. Yang and A.S. Omar, "Rigorous analysis of iris coupling problems in waveguide," *IEEE Trans. Microwave Theory Tech.,* vol. 41, pp. 349–352, 1993.
[13] L. Lewin, *Theory of Waveguides.* New York: Wiley, 1974.
[14] R.E. Collin, *Field Theory of Guided Waves.* New York: McGraw-Hill, 1960.

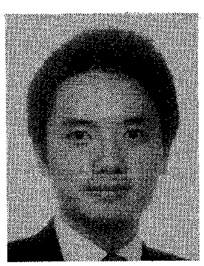

Rong Yang was born in Sichuan, China, on August 30, 1962. He received the B.S. degree in physics from Peking University, Peking, China, in 1983 and the M.S. degree in electrical engineering from University of Electronic Science and Technology of China (UESTC, formerly Chengdu Institute of Radio Engineering), Chengdu, China, in 1986.

From 1986 to 1989 he worked for the UESTC and was promoted to lecturer in 1988. Since 1989 he has been with the Arbeitsbereich Hochfrequenztechnik, Technische Universität Hamburg-Harburg, Hamburg, Germany, where he is now working toward his Ph.D. degree in electrical engineering.

His current research interests are in microwave theory, devices, circuits, and systems.

Abbas S. Omar (M'87–SM'89) received the B.Sc. and M.Sc. degrees in electrical engineering from Ain Shams University, Cairo, Egypt, in 1978 and 1982, respectively, and the Doktor-Ing. degree from the Technische Universität Hamburg-Harburg, Germany, in 1986.

From 1978 to 1982, he served as a Research and Teaching Assistant in the Department of Electronics and Computer Engineering of Ain Shams University, where he was engaged in investigations of microstrip lines and below-cutoff waveguides and their use in a hybrid circuit technique for realizing broad-band tunable oscillators. From 1982 to 1983, he was with the Institut für Hochfrequenztechnik, Technische Universität Braunschweig, Germany, as a Research Engineer, where he was involved with theoretical investigations of finlines. From 1983 to 1987 he held the same position at the Technische Universität Hamburg-Harburg, where he was engaged in investigations of planar structures and dielectric resonators. From 1987 to 1990 he was Senior Research Engineer at the Technische Universität Braunschweig. Since 1990 he has been a Professor of Electrical Engineering and head of the field theory group at the Arbeitsbereich Hochfrequenztechnik, Technische Universtät Hamburg-Harburg. His current fields of research are concerned with optimization of microwave ovens, field analysis of dielectric resonators, analysis and design of three-dimensional passive systems, theoretical investigations of guiding structures, and the design and optimization of planar structures.